Simple all-microstructured-optical-fiber interferometer built via fusion splicing

Joel Villatoro,[1] Vladimir P. Minkovich,[2] Valerio Pruneri,[1,3] and Gonçal Badenes[1]

[1]*ICFO –Institut de Ciencies Fotoniques, Mediterranean Technology Park. Av. del Canal Olimpic s/n 08860 Castelldefels, Barcelona, Spain.*
[2]*Centro de Investigaciones en Optica, A. C., Loma del Bosque 115, C. P. 37150 León Gto., Mexico.*
[3]*ICREA- Institució Catalana de Recerca i Estudis Avançats, 08010, Barcelona, Spain*
joel.villatoro@icfo.es

Abstract: We report a compact and stable all-microstructured-optical-fiber interferometer built with two fusion splices separated a few centimeters from each other. The air-holes of the fiber are intentionally collapsed in the vicinity of the splices. This broadens the propagating optical mode, allowing coupling of two modes in the section between the splices. A truly sinusoidal interference pattern was observed from 800 nm to 1600 nm with fringe visibility reaching 80%. The fringe spacing was inversely proportional to the distance between the splices. The potential of the device for sensing applications is demonstrated.

OCIS Codes: (230.3990) Microstructure devices; (120.3180) Interferometry; (230.1150) All-optical devices; (060.2370) Fiber optics sensors.

References and links

1. P. St. J. Russell, "Photonic-crystal fibers," IEEE J. Lightwave Technol. **24**, 4729-4749 (2006).
2. S. Ghosh, J. E. Sharping, D. G. Ouzounov, and A. L. Gaeta, "Resonant optical interactions with molecules confined in photonic band-gap fibers," Phys. Rev. Lett. **94**, 093902 (2005).
3. F. Benabid, F. Couny, J. C. Knight, T. A. Birks, and P. St J. Russell, "Compact, stable and efficient all-fibre gas cells using hollow-core photonic crystal fibres," Nature **434**, 488-491 (2006).
4. P. J. A. Sazio et. al. "Microstructured optical fibers as high-pressure microfluidic reactors," Science **311**, 1583-1586 (2006).
5. W. N. MacPherson et. al. "Remotely addressed optical fibre curvature sensor using multicore photonic crystal fibre," Opt. Commun. **193**, 97-104 (2001).
6. J. H. Lim, H. S. Jang, K. S. Lee, J. C. Kim, and B. H. Lee, "Mach-Zehnder interferometer formed in a photonic crystal fiber based on a pair of long-period fiber gratings," Opt. Lett. **29**, 346-348 (2004).
7. D. Káčik, I. Turek, I. Martinček, J. Canning, N. Issa, and K. Lyytikäinen, "Intermodal interference in a photonic crystal fibre," Opt. Express **12**, 3465-3470 (2004).
8. J. Ju, W. Jin, and M. S. Demokan, "Two-mode operation in highly birefringent photonic crystal fiber," IEEE Photon. Technol. Lett. **16**, 2472-2474 (2004).
9. R. L. Willing, W. P. Kelleher, and S. P. Smith, "Photonic crystal interferometric fiber optical gyroscope," U.S. Patent Application Publication No: US-2004-0263856, Dec. 30 (2004).
10. J. Villatoro, V. P. Minkovich, and D. Monzón-Hernández, "Compact modal interferometer built with tapered microstructured optical fiber," IEEE Photon. Technol. Lett. **18**, 1258-1260 (2006).
11. L. Yuan, J. Yang, Z. Liu, and J. Sun, "In-fiber integrated Michelson interferometer," Opt. Lett. **31**, 2692-2694 (2006).
12. A. Ozcan, A. Tewary, M. J. F. Digonnet, and G. S. Kino, "Observation of mode coupling in bitapered air-core photonic bandgap fibers," Opt. Commun. to be published.
13. J. H. Chong, M. K. Rao, Y. Zhu, and Y. P. Shum, "An effective splicing method on photonic crystal fiber using CO_2 laser," IEEE Photon. Technol. Lett. **15**, 942-944 (2003).
14. B. Bourliaguet, C. Paré, F. Émond, A. Croteau, A. Proulx, and R. Vallée, "Microstructured fiber splicing," Opt. Express **11**, 3412-3417 (2003).
15. A. D. Yablon, R. T. Bise, "Low-loss high-strength microstructured fiber fusion splices using GRIN fiber lenses," IEEE Photon. Technol. Lett. **17**, 118-120 (2005).
16. C. Kerbage, A. Hale, A. Yablon, R. S. Windeler, and B. J. Eggleton, "Integrated all-fiber variable attenuator based on hybrid microstructure fiber," Appl. Phys. Lett. **79**, 3191-3193 (2001).
17. M. Stevenson, C. Martelli, J. Canning, B. Ashton, and K. Lyytikainen, "Photonic crystal fibre optical attenuators," Electon. Lett. **41**, 1167-1169 (2005).

#77458 - $15.00 USD Received 27 November 2006; revised 16 January 2007; accepted 23 January 2007

18. See for example http://www.crystal-fibre.com/products/termination.shtm
19. V. P. Minkovich, A.V. Kiryanov, A.B. Sotsky, and L.I. Sotskaya, "Large-mode-area holey fibers with a few air channels in cladding: modeling and experimental investigation of the modal properties," J. Opt. Soc. Am. B **21**, 1161-1169 (2004).

1. Introduction

Microstructured optical fibers (MOFs) are characterized by a complex pattern of microscopic air-holes in the transverse plane. Unlike conventional optical fibers, MOFs may be single mode from the visible to the near infrared. In addition, one can design MOFs with multiple cores or with air holes of different shapes [1]. The number, size, shape, and the separation between the air-holes as well as the air-hole arrangement are what confer MOFs their unique guiding mechanism and modal properties [1]. Owing to these properties it is possible to develop novel devices and new scientific or technological applications with microstructured fibers [1-4]. The construction of interferometers with MOFs is of interest and intriguing at the same time owing to the broad range of applications of fiber-based interferometers. To the authors' best knowledge the first attempt to construct an interferometer with an MOF was reported in June of 2001 by Russell's group [5]. They used a dual-core microstructured fiber in which the two cores played the role of arms of the interferometer. Three years later, other novel interferometers constructed with a pair of mechanically-induced long period gratings [6], with a short section of MOF [7], with a Hi-Bi MOF [8], or with photonic band gap fiber [9] were reported. More recently, it has been demonstrated that MOFs combined with tapering technology allow the construction of compact interferometers with interesting features [10-12]. One thing that the interferometers reported in [6]-[8], [10], and [12] have in common is that the "arms" of the interferometers are typically two modes. In order to excite two modes in a MOF one may use long period gratings [6], critical launching and polarization conditions [5,7,8], or tapering techniques [10-12]. All these techniques present challenges in terms of complexity and/or manufacturability and thus in this work we address the construction of simple and stable interferometers with microstructured optical fiber via fusion splicing.

It is known that when splicing together two MOFs, or a MOF and a conventional optical fiber, with the standard electric-arc method, the air-holes of the MOF collapse completely in the vicinity of the splice [13-15]. The collapsing of the voids in a short region of the MOF (considered problematic in the past [13,14]) is not a serious drawback of fusion splices since it may introduce minimal losses [15,16]. In addition, the collapsing of the microscopic air-holes is exploited to design useful all-MOF devices such as filters [1], attenuators [17], or especial pathcords [18]. The cleaving and splicing processes take a few minutes and can be carried out with standard fiber optics equipment. The collapsing of the voids in a short region makes the fundamental MOF mode to spread out. Thanks to this phenomenon it is possible to excite the core and higher order modes in the section of MOF between the splices. Such modes propagate at different phase velocities, thus in a certain length of MOF the modes accumulate a differential phase shift. Since the phase velocities and the phase difference are wavelength dependent, the optical power transmitted by the device will be maximum at certain wavelengths and minimum at others. The interferometers we fabricated exhibited truly sinusoidal and stable interference spectra which were observed over a broad wavelength range (~800 nm). The period of the devices was found to be inversely proportional to the length of MOF between the two splices.

Interferometers with microstructured fibers are attractive since they can have a significant impact in optical sensing and communications. Here the potential of our interferometer for optical sensing is demonstrated experimentally. Other applications such as mode or wavelength filtering seem also feasible.

#77458 - $15.00 USD Received 27 November 2006; revised 16 January 2007; accepted 23 January 2007

2. Device fabrication and results

For the construction of microstructured Mach-Zehnder interferometers we employed a home-made MOF consisting of a solid core surrounded by four rings of air holes arranged in a hexagonal pattern [19]. Such a fiber had a core of 11 μm in diameter, voids with average diameter of 2.7 μm, and the average separation between the voids was 5.45 μm. This index-guiding fiber is single mode from 620 nm to 1600 nm [19]. An atomic force microscope image of our MOF and a micrograph of one of the splices that formed one of our interferometers are shown at the top of Fig. 1. The drawing in the bottom of the figure is a schematic illustration of the all-MOF interferometer in which the splices are represented by white areas. The center-to-center separation between the splices is denoted as L.

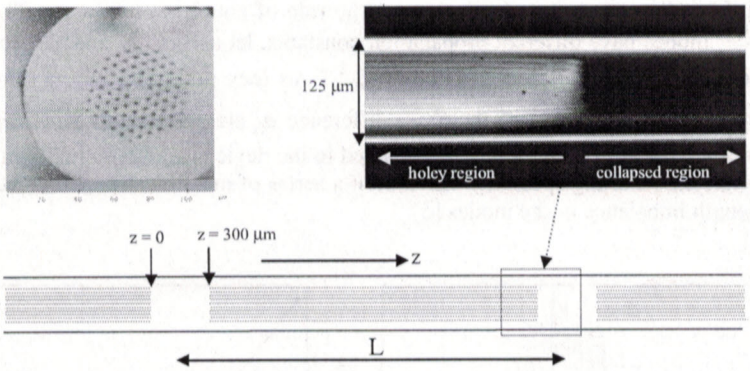

Fig. 1. Atomic force microscope image of the MOF used in the experiments (top-left image) and a micrograph of a section of the MOF splice (top-right image). The bottom drawing is a schematic representation of the all-MOF interferometer. The splices are illustrated as white areas, the horizontal lines represent the holey region of the MOF, L is the separation between the splices, and z represents the direction of propagation.

In all the samples we fabricated the splices were carried out with a conventional fusion splicer (Fitel S122A). Before splicing the fibers we cleaved them with a high-precision cleaver (Fitel model S325). All the splices were carried out under similar conditions. To minimize the losses and to achieve robust splices we reduced the default (for standard single mode fiber) heating time and current of the electrodes of the splicer by approximately 50%. Note from the image of Fig. 1 that the air channels of the MOF (the horizontal lines of the micrograph) are tapered before being completely collapsed. Also, that the outer diameter of the MOF is basically uniform even in the region with collapsed air channels. The full length of each collapsed zone including both sides of the splice was ~300 μm. The fabrication of the interferometers was monitored *in situ* and in real time. To do so we employed an LED centered at 850 nm and a spectrometer. It should be pointed out that the losses of each splice (at 850 nm) were less than 5 dB. We believe that such losses can be further reduced with an optimization of the splicing program. Such an optimization is in progress.

To understand the behavior of the interferometer let us consider the evolution of the fundamental mode at the first splice as it travels from the holey region to the solid region. The fundamental MOF mode immediately begins to diffract since it reaches a piece of coreless fiber, see Fig. 1. Owing to the diffraction the mode broadens. Such a broadening can be estimated by using a Gaussian beam approximation [15]. According to it the fiber's mode field diameter (MFD) at any z (the direction of propagation) depends on the wavelength (λ) of the guided light, the refractive index n_1 of the medium (pure silica in our case), and the light spot size (ω_0) as:

#77458 - $15.00 USD Received 27 November 2006; revised 16 January 2007; accepted 23 January 2007

$$\mathrm{MFD} = 2\omega_0\sqrt{1+(z\lambda/n_1\pi\omega_0^2)^2}\ . \qquad (1)$$

If we assume that the solid region starts at z = 0, see Fig. 1, then at the end of the solid region, i.e., at z = 300 μm, according to Eq. (1), the MFD practically triplicates when λ = 1.55 μm and doubles when λ = 0.85 μm. This means that the enlarged mode does not reach the surface of the collapsed region and it is therefore insensitive to the external medium. At z ~300 μm the mode reaches a piece of MOF of length L (in our case L is less that 13 cm). We believe that in such a short fiber the fundamental core mode and a higher order mode are excited. This reasoning is based on the fact that two modes are typically supported in short lengths of fiber [7]. The two excited modes are enlarged and "recombined" by the second splice. In this interferometer the excited modes in the piece of MOF between the splices play the role of arms and the collapsed regions (splices) play the role of couplers or splitters. The core and higher order modes have different propagation constants, let us say, β_1 and β_2, respectively, and accumulate a phase difference $\phi_{12} \equiv (\beta_1 - \beta_2)\cdot \mathrm{L}$ as they propagate over a length L. The propagation constants β_1, β_2, and the phase difference ϕ_{12} are wavelength dependent. Thus, if light from a broadband optical source is launched to the device and the output light is fed to a spectrometer; the resulting spectrum will exhibit a series of maxima and minima according to the path length imbalance of the modes [5].

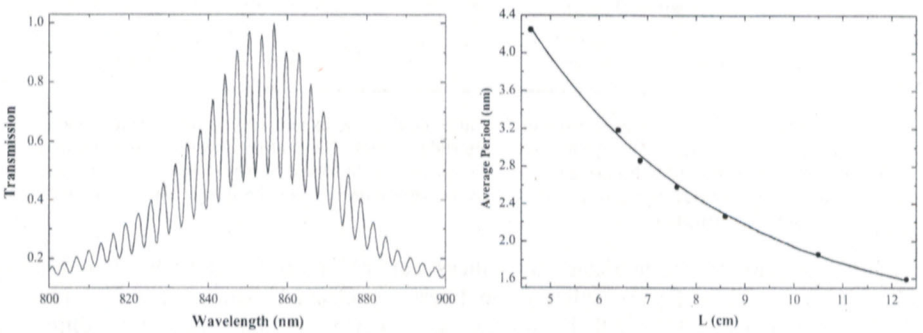

Fig. 2. (left) Experimental normalized transmission spectrum around 850 nm of a MOF interferometer with L = 6.35 cm. (right) Average period of the interferometers versus the length L of MOF between the splices. The dots are experimental points and the continuous line is an exponential fitting to the points.

In the left-hand side plot of Fig. 2 we show the normalized transmission spectrum of an interferometer with L = 6.35 cm constructed with the MOF described above. The visibility of the fringes was ~40%. To obtain the interference spectrum shown in the figure we used as a light source a low-power LED with peak emission at 850 nm and 50 nm of spectral width. The output light was fed to a miniature optical spectrum analyzer (Ocean Optics USB4000) that was attached to a personal computer in which the data were analyzed and stored. The interference spectrum has a Gaussian-like envelope owing to the output spectrum of the LED. Several interferometers with different L's were fabricated. As expected the interference fringes became closer as L increased. The right-hand side plot of Fig. 2 summarizes our results. For L's bigger that ~14 cm we did not observe interference. The higher order mode is highly lossy and therefore it is lost through radiation leakage [7]. It should be pointed out that during the measurements the section of fiber between the splices was held straight since the interference pattern was strongly affected by bending. In this regard, our interferometer is similar to those constructed with dual-core MOFs [5,11].

#77458 - $15.00 USD
Received 27 November 2006; revised 16 January 2007; accepted 23 January 2007

Like any other two-mode interferometer the fringe period (Λ) of our devices at any λ can be calculated by means of the expression:

$$\Lambda = \frac{2\pi\lambda}{(\beta_1 - \beta_2)\cdot L}. \quad (2)$$

Knowing the modes involved in the interference (i.e., β_1 and β_2) one can calculate Λ. Conversely, the knowledge of L, λ, and Λ helps to calculate $\Delta\beta = \beta_1 - \beta_2$. From Fig. 2 $\Delta\beta$ was calculated to be $\Delta\beta \approx 2.74\text{x}10^{-5}\,\text{nm}^{-1}$.

The interferometers were also tested at longer wavelengths, in the near-infrared region of the spectrum, up to 1600 nm. Since most MOFs exhibit single mode behavior in a broad range of wavelengths it was natural to expect interference effects at wavelengths longer than 850 nm. For this purpose we used a tunable laser (Photonetics) as a light source and measured the output optical power with an InGaAs photodetector (OZ Optics). In Fig. 3 we show the normalized transmitted power of an interferometer with L = 7.5 cm as a function of the wavelength. A series of maxima and minima are also observed at wavelengths around 1510 nm. The sinusoidal interference pattern shown in Fig. 3 indicates that only two modes are interfering which justifies the earlier discussion. The fringe visibility was calculated to be ~80%. The visibility is higher than that of Fig. 2 because of the coherence of the 1500 nm laser is higher than that of the 850 nm LED. The average period of the interference spectrum shown in Fig. 3 is 3.1 nm. Note from Fig. 2 that the period at 850 nm of a device with L = 7.5 cm is 2.6 nm. These results agree well with Eq. (2) which indicates that the period of all-MOF interferometers constructed with splices increases with the wavelength.

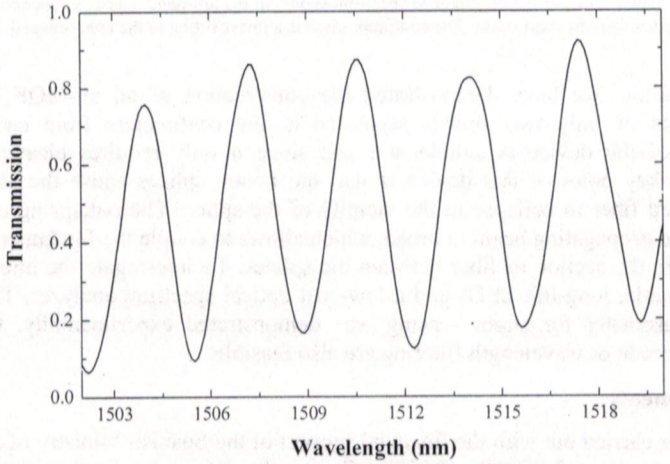

Fig. 3. Normalized transmission versus wavelength of an interferometer with L = 7.5 cm. The light source was a tunable laser and the output power was measured with an InGaAs photodetector.

3. Device applications and conclusions

The interferometer discussed here can have diverse applications. For example, if by some means ϕ_{12} or L are modified, the interference pattern will change or shift. This property can be exploited for optical sensing. We found that the interference pattern shifted to shorter wavelengths when the interferometer was subjected to longitudinal strain. Therefore, we explored the application of our devices for strain sensing. We used an interferometer with L = 8.6 cm. To introduce micro elongations to the device we secured it between two displacement

#77458 - $15.00 USD Received 27 November 2006; revised 16 January 2007; accepted 23 January 2007

mechanical mounts that were separated 8 cm. With this we ensured that only the section of MOF between the splices was subjected to the applied strain. In the left-hand graph of Fig. 4 we show the interference pattern of the referred interferometer at 0 με (continuous line) and at 750 με (dotted line). The right-hand graph of Fig. 4 shows the shift of the left-hand interference spectrum as a function of the applied (squares) or removed (crosses) strain. It is worth noting the linear behavior of the device as well as its reversibility. Other sensing applications of the interferometer discussed here can be envisaged since many physical parameters such sound, vibration, temperature, pressure, etc., can be transduced to strain changes. The potential application of the all-MOF interferometers presented here for wavelength filtering (see Fig. 3) seems also feasible.

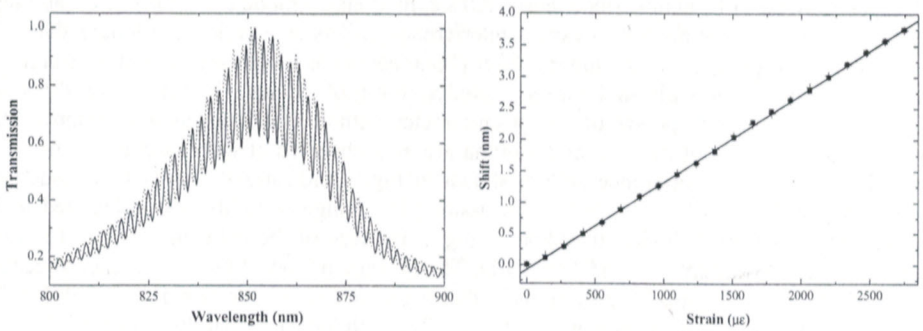

Fig. 4. (left) Interference spectra of an interferometer with L = 8.6 cm subjected to 0 (solid line) and 750 με (dotted line). (right) Shift of the interference spectrum shown in the left-hand side as a function of the applied (squares) or removed (crosses) strain. The continuous line is a linear fitting to the experimental data.

In conclusion, we have demonstrated the construction of an all-MOF interferometer which consists of only two splices separated a few centimeters from each other. The construction of the device is simple and fast since it only requires cleaving and fusion splicing. The key point of this device is that the fusion splices cause the air-holes of the microstructured fiber to collapse in the vicinity of the splice. The collapsing of the voids in turn makes the propagating beam to broad, which allows to couple the fundamental and higher order modes in the section of fiber between the splices. To interrogate the interferometer we employed reliable, long-life LEDs and a low-cost optical spectrum analyzer. The application of the interferometer for strain sensing was demonstrated experimentally. Other sensing applications, mode or wavelength filtering are also feasible.

Acknowledgments

This work was carried out with the financial support of the Spanish Ministry of Education and Science through grant TEC2006-10665/MIC and the European Commission through the European Network of Excellence PHOREMOST (FP6-511616). The authors are also grateful to the Consejo Nacional de Ciencia y Tecnología (Mexico) for financial support under project No. 42986-F. Joel Villatoro acknowledges funding from the Ministerio de Educación y Ciencia (Spain) through the "Ramón y Cajal" program.

#77458 - $15.00 USD
Received 27 November 2006; revised 16 January 2007; accepted 23 January 2007